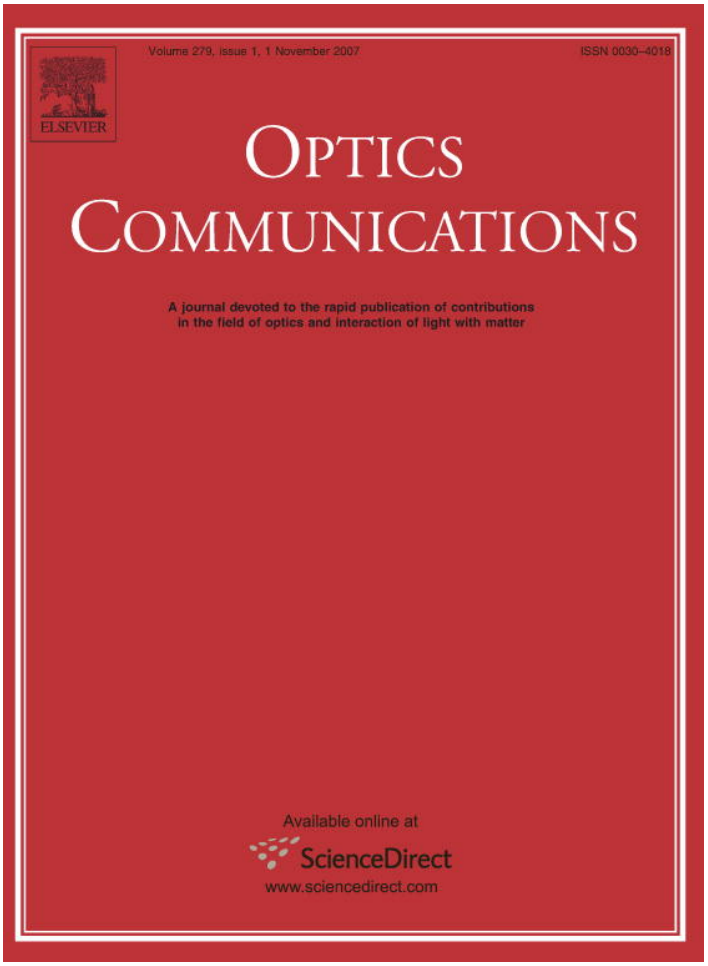

Available online at www.sciencedirect.com
ScienceDirect
Optics Communications 279 (2007) 196–202
OPTICS COMMUNICATIONS
www.elsevier.com/locate/optcom

Quasi-stable propagation of vortices and soliton clusters in saturable Kerr media with square-root nonlinearity

Miroslav M. Petroski [a,b], Milan S. Petrović [a,*], Milivoj R. Belić [a,c]

[a] Institute of Physics, P.O. Box 57, 11001 Belgrade, Serbia
[b] High School Čede Filiposki, 1230 Gostivar, Macedonia
[c] Texas A&M University at Qatar, P.O. Box 5825, Doha, Qatar

Received 15 April 2007; received in revised form 4 July 2007; accepted 6 July 2007

Abstract

Analytical and numerical investigation of the propagation of optical beams in Kerr-like saturable photorefractive media is carried out, utilizing a novel model for the local isotropic part of the space-charge field generated in the medium. Using a variational technique, optimal propagation parameters for the most stable propagation of otherwise unstable single Gaussian, single vortex, and optical soliton cluster beams are determined. Analogy between a ring of identical weakly overlapping solitons and a vortex of the same topological charge is explored.

PACS: 42.65.Tg; 42.65.Sf

1. Introduction

Progress in generating spatial optical solitons in nonlinear (NL) bulk media opens the possibility of intense study of two-dimensional (2D) interaction and self-trapping of light beams [1]. Spatial solitons display robust nature in interactions [2], thus a formal analogy with the atomic physics can be established and spatial solitons can be treated as the ''atoms of light.'' Using a certain number of simple solitons (or ''atoms'') one can construct more complex objects, multisoliton bound states (or ''optical atom clusters'') in a homogeneous bulk NL optical medium. Self-trapped azimuthally periodically modulated beams (''necklace beams'') can exist in such media, exhibiting quasi-stable expansion even in a self-focusing NL medium [3–5]. Because of zero angular momentum they do not manifest rotation during propagation.

The major problem in these studies is inherent instability of beam propagation in NL self-focusing optical media [6]. Solitonic structures propagating in such media often possess internal modes and tend to develop modulational instabilities (MI) which lead to the breakup of simple beam arrangements into more complex ones. The idea then is to harness these internal modes and MI to achieve more stable propagation of complex beam structures. Competition between different optical nonlinearities is very important for the improvement of the stability of single vortex solitons and 2D and 3D soliton clusters [7–9]. The key physical mechanism for soliton cluster stabilization is associated with a staircase-like phase distribution that induces a net angular momentum and leads to quasi-stable cluster rotation [10–12].

It has recently been pointed out that the inclusion of spatial nonlocality into NL propagation may arrest collapse and improve the stability of light beams [13]. Nonlocal response provides a mechanism for the stabilization of solitonic clusters and azimuthally modulated vortex beams [14]. In this paper, we explore an alternative way to improve stability, by staying within the local approximation but using a more appropriate model for the generation of space-charge field in homogeneous photorefractive (PR)

* Corresponding author.
E-mail address: petrovic@phy.bg.ac.yu (M.S. Petrović).

0030-4018/$ - see front matter © 2007 Elsevier B.V. All rights reserved.
doi:10.1016/j.optcom.2007.07.006

crystals. These are the media of choice for the study of quasi-stable propagation of more complex solitonic beam structures. Generally, such structures are metastable (i.e., in the absence of any perturbations they propagate stably over many diffraction lengths in a saturable medium, experiencing spontaneous symmetry-breaking instability only at the end). We are looking into ways of extending this quasi-stable regime of propagation, by exploring improved modeling of PR media. We are also looking into similarities between rings of identical weakly overlapping solitons carrying orbital angular momentum and vortices of the same topological charge.

To this end we utilize an isotropic model of PR media with a local interaction of beams that is specifically suitable for transverse 2D geometries. The model, developed in [15,16], contains a more realistic expression for the PR space-charge field, of the form:

$$E_{sc} = E_0 \frac{1}{\sqrt{1+I}}, \tag{1}$$

where E_0 is the transverse dc electric field applied to the PR crystal, to induce the formation of the space-charge field, and I is the total beam intensity measured in units of the dark or background intensity. The square-root intensity dependence represents more accurately the most relevant isotropic contribution to the space-charge field and constitutes an improved model to be used for describing the propagation of $(2+1)$D spatial screening solitons. It offers more accurate results in comparison to the straightforward generalization of the 1D formula $1/(1+I)$, which is used by most authors. In addition, as it will be seen, it leads to improved stability of propagating complex optical structures and longer propagation distances.

The equation for the slowly varying optical field envelope E can be written in the form of the general dimensionless nonlinear Schrödinger equation:

$$\mathrm{i}\frac{\partial E}{\partial z} + \Delta_\perp E + f(I)E = 0, \tag{2}$$

where $\Delta_\perp$ is the transverse Laplacian and z is the propagation distance, measured in the units of the diffraction length L_D. The function $f(I) = -1/\sqrt{(1+I)}$ describes NL properties of the PR optical medium, and depends on the total beam intensity $(I = |E|^2)$ only.

Following the standard procedure, the Lagrangian and Hamiltonian densities of the root model are easily found

$$\mathscr{L} = \frac{\mathrm{i}}{2}\left(E\frac{\partial E^*}{\partial z} - \text{c.c.}\right) + |\nabla_\perp E|^2 + 2\sqrt{1+|E|^2}, \tag{3}$$

$$\mathscr{H} = \frac{\mathrm{i}}{2}(E\partial_z E^* - \text{c.c.}) - \mathscr{L}. \tag{4}$$

Hamiltonian and the action can be written as usual

$$H = -\int \left\{|\nabla_\perp E|^2 + 2\sqrt{1+|E|^2}\right\}\mathrm{d}x\,\mathrm{d}y, \tag{5}$$

$$S = \int \mathscr{L}\,\mathrm{d}\mathbf{r}_\perp. \tag{6}$$

We utilize these quantities in describing the propagation of various beam structures in the medium. The procedure is to determine optimal parameters for different beam structures utilizing variational principles, then launch optimized beams into the medium, and observe the subsequent behavior.

2. Single Gaussian

We consider first a Gaussian-like solution, described by an input ansatz:

$$E = A\exp(-(x^2+y^2)/2a^2), \tag{7}$$

where x and y are dimensionless coordinates in the transverse plane (scaled by the typical width of beams used in experiments) and a (the width) and A (the amplitude) are the parameters to be optimized. Optimal values of these parameters can be found from the principle of minimum action.

The main quantity characterizing a spatial soliton is its power:

$$P = \int |E|^2 \mathrm{d}\mathbf{r}_\perp = \pi a^2 A^2, \tag{8}$$

which is dimensionless here, and represents an integral of motion. The variational conditions $\delta S/\delta A = \delta S/\delta a = 0$ for finding the parameters of a single soliton, described by the ansatz (7), give only one relation betwen a and A:

$$\int_{-\infty}^{\infty}\int_{-\infty}^{\infty} \frac{\left[\frac{(x^2+y^2)}{a^2} - 1\right]\mathrm{e}^{-\frac{x^2+y^2}{a^2}}}{\sqrt{1+A^2\mathrm{e}^{-\frac{x^2+y^2}{a^2}}}}\mathrm{d}x\mathrm{d}y - \pi = 0, \tag{9}$$

so, instead of only one solution, we have an infinite number of solutions, Fig. 1. Eq. (9) can be analytically solved only in the small amplitude approximation (valid for a large beam width), and we find $P \equiv \pi a^2 A^2 \to 8\pi$.

Gaussian-like solutions represent very stable but pulsating (breathing) solitons. Oscillations in the transverse directions are the smallest for the points on the curve, defined by Eq. (9).

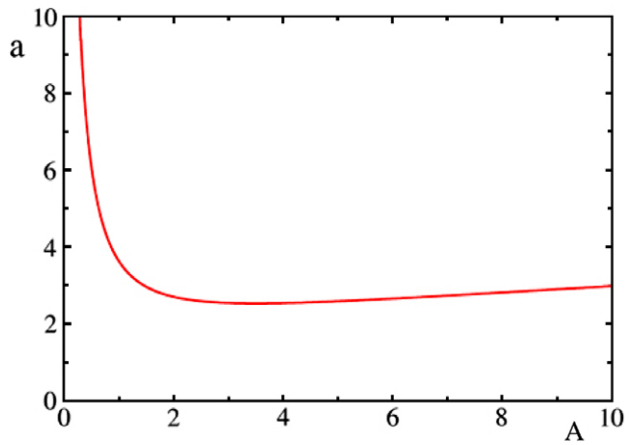

Fig. 1. Solution of Eq. (9) for the parameters of Gaussian-like solitons.

3. Single vortex

Next, we consider a vortex-like solution, described by the ansatz:

$$E(\rho,\varphi) = A\rho e^{-\frac{\rho^2}{2a^2}} e^{im\varphi}, \tag{10}$$

where (ρ,φ) are the polar coordinates in the transverse plane and m is the topological charge. The beam power is equal to

$$P = \int |E|^2 d\mathbf{r}_\perp = \pi a^4 A^2. \tag{11}$$

The variational conditions $\delta S/\delta A = \delta S/\delta a = 0$ for finding optimal parameters a and A of a single vortex soliton give again only one equation:

$$\int_0^\infty \frac{\frac{\rho^2}{a^2}\left[\frac{\rho^2}{a^2}-2\right]e^{-\frac{\rho^2}{a^2}}}{\sqrt{1+\rho^2A^2e^{-\frac{\rho^2}{a^2}}}}\rho d\rho - \frac{(1+m^2)}{2} = 0. \tag{12}$$

Characteristic solutions of this equation are shown in Fig. 2, with the behavior similar to Gaussian beams. As before, Eq. (12) can be solved analytically only in the small amplitude region (where the beam width is large), and we find $P \equiv \pi a^4 A^2 \to 16\pi(1+m^2)$.

Vortices oscillate during propagation in such a way that the power (11) is always conserved. For $m = 1$, a single vortex with the parameters above the corresponding curve of Fig. 2 oscillates anharmonically with very small amplitude, and disintegrates into concentric rings. A single vortex with parameters below the curve oscillates harmonically with an amplitude that increases with the increasing distance from the curve, and fragments into several fundamental solitons that fly tangentially off the ring.

For a given beam power P, a single vortex propagates in the most stable fashion (the harmonic oscillations are the smallest) if the parameters are determined by Eq. (12). In this case, the vortex width a oscillates about its mean value by about 10%. The quasi-stable propagation distance depends on P, and above the beam power threshold, it increases with the increasing beam power. For example, a vortex of unit topological charge with $P = 3\times10^8$ propagates stably until 4800 L_D. We define the stable propagation length as the propagation distance at which the symmetry-breaking instabilities start to develop.

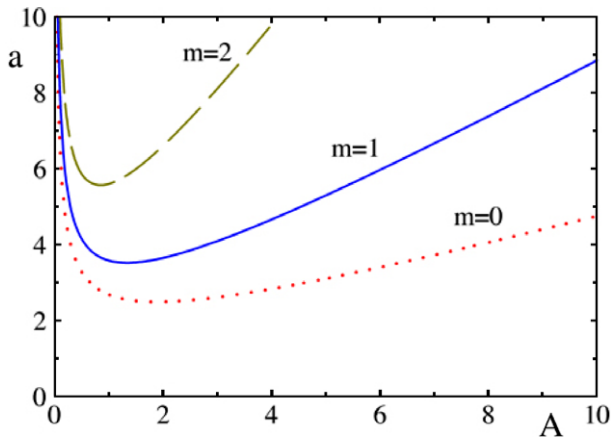

Fig. 2. Solution of Eq. (12) for the vortices with different values of the topological charge m.

For vortices with the topological charge $m = 1$ it is possible to find the period of oscillations

$$T = \frac{\pi}{\sqrt{2}} a_{(0)}^2, \tag{13}$$

where $a_{(0)} = a\,(z = 0)$ is the input value of optimized a. This relation holds only for the points on the curve given in Fig. 2, which are to the right of the curve minimum.

4. Soliton clusters

We now consider situations where more than one beam is launched into the crystal. We build onto the concept of necklace beams developed in [3–6,10,11], extending it to the root model, and in the process demonstrate that the quasi-stable propagation distances increase for an order of magnitude over the distances achieved in the inverse-intensity saturable model.

In the simplest case of two coherent spatial solitons, the interaction between them depends on the relative soliton phase difference θ: two solitons attract each other for $\theta = 0$, and repel each other for $\theta = \pi$. For intermediate values of the soliton phase, energy exchange and inelastic interaction between the solitons become the most dominant effects. From the geometrical considerations it is clear that the only structures suitable for balancing the phase-sensitive coherent interaction between neighboring solitons should possess a ring-like geometry. However, due to tension induced by the bending of the soliton array, this configuration will be (in general) radially unstable: a ring of N solitons will expand if the mutual interaction between the neighboring solitons is repulsive, or otherwise collapse. Effective centrifugal force, in the form of an additional phase of the scalar field that twists by $2\pi m$ along the soliton ring, can balance out the tension effect and stabilize the ring-like soliton cluster. This leads to the cluster rotation, with an angular velocity which depends basically on the phase charge m.

To describe soliton clusters analytically, we consider a coherent superposition of N solitons with the beam envelopes $G_n(x,y,z)$, $n = 1,2...,N$, propagating in a homogeneous bulk saturable Kerr-like medium where the total optical field is $E = \sum G_n$. For a ring of identical weakly overlapping solitons launched in-parallel, we can employ the Gaussian ansatz for the single beam G_n [6,10]:

$$G_n = A\exp\left(-\frac{|\mathbf{r}-\mathbf{r}_n|^2}{2a^2} + i\alpha_n\right), \tag{14}$$

where $\mathbf{r}_n = \{x_n; y_n\} = \left\{R\cos(\frac{2\pi n}{N}); R\sin(\frac{2\pi n}{N})\right\}$ defines the soliton's initial location, R is the ring radius, and $\alpha_n = \theta n = \frac{2\pi m}{N} n$ is the phase of the nth beam. The number

m plays the role of a topological charge of the corresponding phase dislocation associated with the ring. The quantity $\theta = 2\pi m/N$ is the relative phase between the two neighboring solitons in the ring.

Our aim is to propagate a ring-like configuration of N coherently interacting solitons for as long as possible. To this end we first determine the parameters for ring components: the idea is to construct the most robust possible single solitons, using the variational technique, by finding the best propagation parameters a and A (Fig. 1). Then it is necessary to specify the parameters which characterize the ring: the radius R and the topological charge m. To do so, we substitute the ansatz (14) into the relation for the effective interaction potential $U(R)$ (or the normalized system's Hamiltonian) [10]

$$U = -\int \left\{ |\nabla_\perp E|^2 + 2\left(\sqrt{1+|E|^2} - 1\right)\right\} \mathrm{d}x\,\mathrm{d}y, \tag{15}$$

and plot U as a function of R. The minimum of this function at a finite value of R (denoted here as R_0) will indicate the most stable cluster configuration against the collapse or expansion.

In saturable Kerr media with the square-root nonlinearity, for $N \geqslant 4$ we can see three distinct types of the interaction potential $U(R)$. Only one of them has a local minimum at finite R, the other two types of the effective interaction potential are attractive and repulsive. The particular case $N = 10$ is shown in Fig. 3. The effective potential is always attractive for $m = 0$. For $4 \leqslant N < 8$ the dynamically stable bound states are possible for $m = 1$ only, while for $N \geqslant 8$ they exist for $m = 1$ and $m = 2$. The effective interaction potential is always repulsive for higher values of m. The stability of such soliton clusters during propagation is tested numerically.

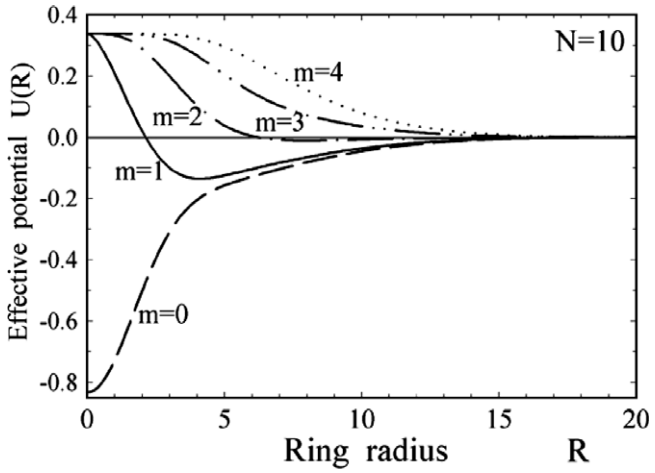

Fig. 3. Effective interaction potential $U(R)$ for a cluster of $N = 10$ solitons (with single soliton parameters $A = 3.503$ and $a = 2.530$). Dynamically stable bound states are possible for values of the topological charge $m = 1$ ($R_0 = 4.12$) and $m = 2$ ($R_0 = 7.94$) .

5. Numerical results

Here, we present results obtained by numerical solution of Eq. (2). We execute a series of numerical simulations of different N-soliton rings, using a beam propagation method based on the fast Fourier transform technique. We find excellent agreement between observed numerical cluster dynamics and our analytical analysis founded on the effective-particle approach, although the numerical ring dynamics tends to be more complicated.

Different interaction scenarios for a cluster of $N = 10$ solitons are shown in Fig. 4. The first column presents the case with $m = 0$; because of the zero angular momentum the cluster does not exhibit rotation during propagation. The effective interaction potential is attractive, and the collapse and fusion through oscillations are observed. In the second and third columns stationary bound states are presented that correspond to the minima of the effective interaction potential $U(R)$ in Fig. 3, for $m = 1$ and $m = 2$. The soliton attraction is balanced by the repulsive centrifugal force, and the clusters preserve their form, while rotating, during the propagation. The cluster with $m = 1$ propagates longer; reasons being the larger centrifugal force in the $m = 2$ case (i.e., the larger angular momentum) and the shallower effective interaction potential. The fourth column in Fig. 4 represents an example of soliton repulsion, with $m = 3$: although strongly overlapping in the beginning, the single solitons preserve their individuality during the cluster expansion.

Different rotating soliton clusters, as well as azimuthal MI developing in these systems, are presented in Fig. 5. As demonstrated earlier [17,18], optical solitons carrying orbital angular momentum are unstable in propagation, breaking into filaments, which develop into solitons, whose number is dependent on the input angular momentum. After a symmetry-breaking instability, the solitons fly out tangentially from the initial ring, like free Newtonian particles. Interestingly, generally metastable clusters initially always rotate more than one full rotation (but less than two!), then energy exchange between solitons takes place and the filamentation occurs, but the filaments (which become flying solitons) rotate in the opposite direction (Fig. 5).

As a consequence of the nonstationary behavior during cluster propagation (such as breathing and emitting radiation), cluster's radius is not a constant quantity. To investigate cluster oscillations, we monitor the cluster's mean radius $\langle R \rangle$, given by the formula:

$$\langle R(z) \rangle = \frac{1}{P} \int\int \sqrt{x^2 + y^2} |E|^2 \mathrm{d}x\,\mathrm{d}y. \tag{16}$$

The evolution of cluster's mean radius $\langle R \rangle$ as a function of the propagation distance is shown in Fig. 6. Input cluster radius $R_0 = 4.25$ corresponds to the minimum of the effective interaction potential $U(R)$ (Eq. (15)), for a cluster of $N = 8$ solitons and with the topological charge $m = 1$. As it can be seen in Fig. 6, the cluster with the input radius

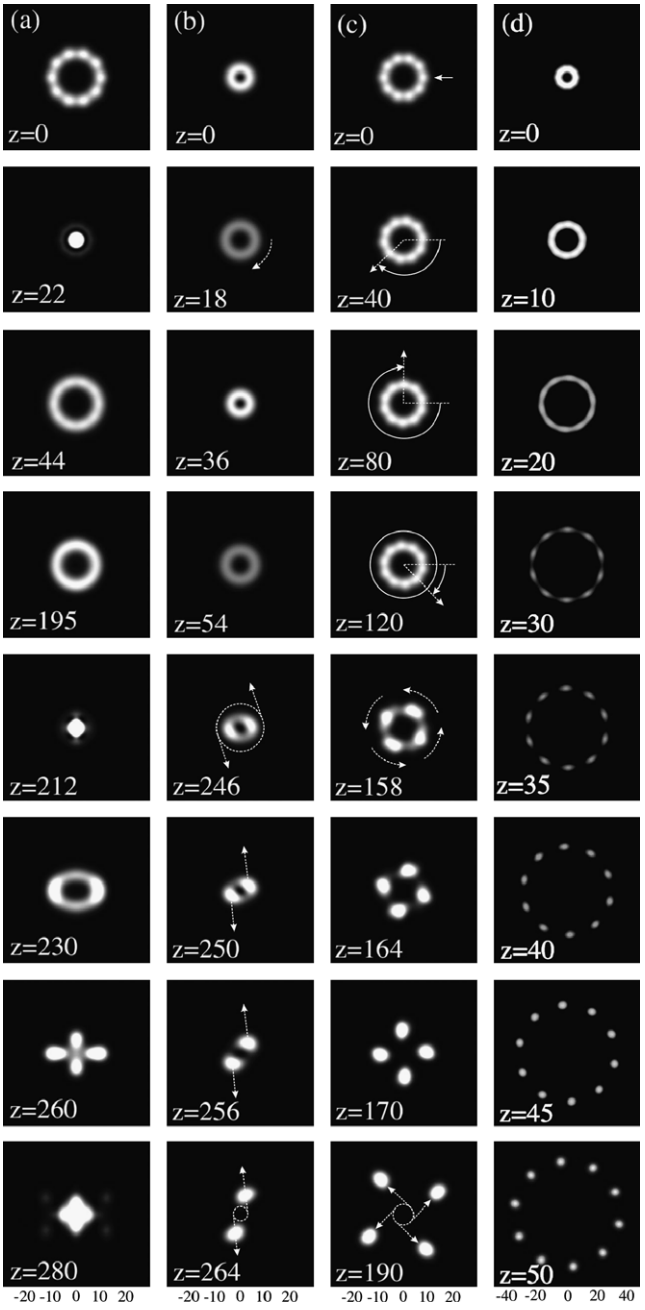

Fig. 4. Different interaction scenarios for a cluster of $N = 10$ solitons: (a) $m = 0$, collapse and fusion through oscillations, input cluster radius is $R = 10$; (b) $m = 1$, stationary bound state with $R_0 = 4.12$; (c) $m = 2$, stationary bound state with $R_0 = 7.94$; (d) $m = 3$, soliton repulsion, $R = 5$.

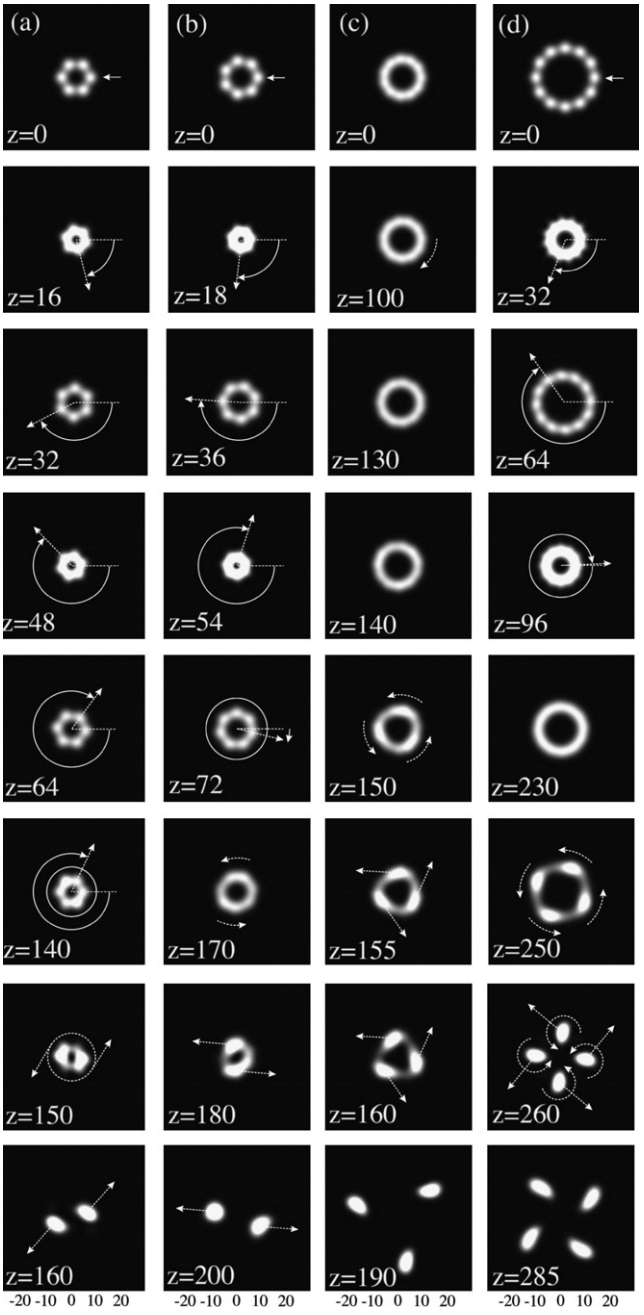

Fig. 5. Rotating soliton clusters: (a) $N = 6$, $m = 1$, input cluster radius is $R = 6$; (b) $N = 7$, $m = 1$, $R = 7$; (c) $N = 11$, $m = 2$, stationary bound state with $R_0 = 7.61$; (d) $N = 12$, $m = 2$, $R = 12$. Arrows indicate the direction of rotation; for the last two rows, arrows show the trajectories of the flying solitons, after the instability-induced splitting.

R_0 does not oscillate about this value during propagation: we find that it oscillates about the radius $R = 4.75$. To reduce cluster oscillation we choose input cluster radius $R = 4.75$, and also obtain longer propagation distance (as expected). For other values of R (for example, $R = 8$), the amplitude of the cluster oscillation is greater (Fig. 6). In all three cases the clusters propagate to a similar distance, because the propagation length mostly depends on the beam power. These distances favorably compare with the distances obtained by other models [11,12]. The nonlinearity model used in [11] is with the inverse saturable intensity, whereas the one in [12] is of the cubic-quintic type.

6. Propagation distance and beam power

There exists a significant analogy between a ring of identical weakly overlapping solitons carrying orbital angular momentum and a vortex of the same topological charge, Fig. 7. Vortices and clusters oscillate in a similar fashion during propagation; their amplitudes and widths oscillate

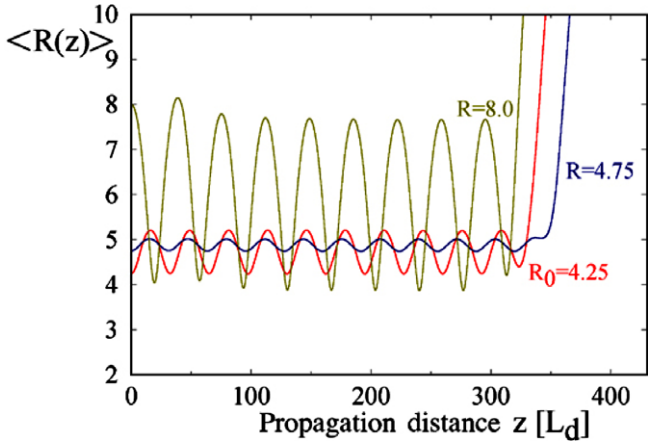

Fig. 6. Cluster's mean radius $\langle R \rangle$ as a function of the propagation distance z, for three different values of the input cluster radius. Parameters: $N = 8$, $m = 1$.

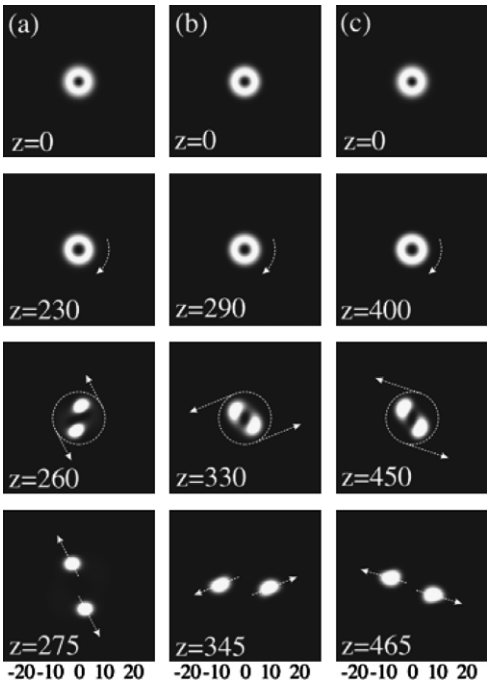

Fig. 7. Propagation of vortices and soliton clusters with the same input radius and topological charge $m = 1$, but with different beam powers: (a) vortex with the beam power $P = 217$ ($A = 0.46$, $a = 4.25$); (b) cluster with $P = 1974$ ($N = 8$, a stationary bound state with $R_0 = 4.25$); (c) vortex with $P = 11162$ ($A = 3.30$, $a = 4.25$). Vortex parameters are chosen from Fig. 2.

with the opposite phases, because of the beam power conservation. For both single vortices and soliton clusters, the propagation distance is longer for smaller amplitude oscillations and greater beam powers (Fig. 7), while the phase distributions are very similar.

The quasi-stable propagation distance does not have to always increase with the increasing beam power. Fig. 8 displays the propagation distance as a function of P for vortices and soliton clusters of $N = 6$ solitons, with the same topological charge $m = 1$. For $P \cong 400$, one can notice a

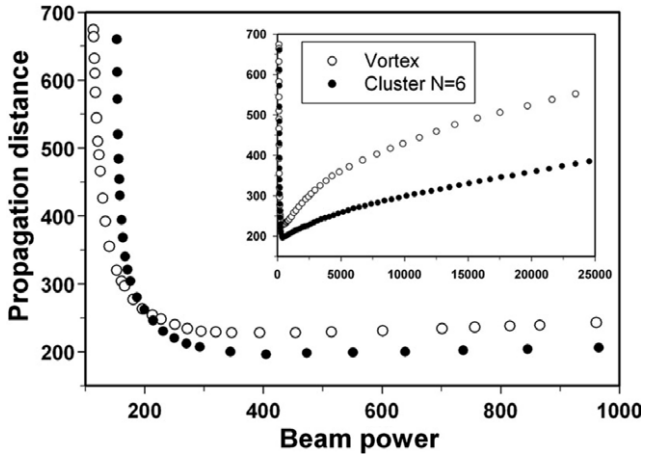

Fig. 8. Propagation distance as a function of beam power for vortices (empty circles) and clusters of $N = 6$ solitons (filled circles), with the same topological charge $m = 1$. Vortex parameters are chosen from Fig. 2. Individual solitons parameters are chosen from Fig. 1, while input cluster's radii are determined as values corresponding to the minima of the effective interaction potential.

beam power threshold: above/below it, the propagation distance increases with the increasing/decreasing P. The parameter region below the beam power threshold corresponds to small amplitudes and large beam widths, and the propagation distances tend to very big values, while the beam power approaches its minimum (32π for vortices, and 48π for clusters of $N = 6$ solitons). Propagation distance minima are different for the two cases ($\sim 230 L_D$ for vortices, and $\sim 200 L_D$ for soliton clusters).

7. Conclusions

We investigated analytically and numerically the propagation of optical beams in nonlinear PR media. We utilized a novel isotropic model for the generation of space-charge field in PR media with local interaction of beams, that is specifically useful for transverse 2D geometries. To observe long-term quasi-stable dynamics, we determined optimal propagation parameters for single Gaussian, single vortex, and optical soliton cluster beams, using a variational technique. We found excellent agreement between numerics and our predictions, based on the principle of minimum action, in the cases of vortices and weakly overlapping soliton rings. Because the ring-like soliton cluster is a discrete generalization of the vortex soliton, we explored analogy between them. We obtained that vortices and soliton clusters suffer azimuthal instability and fragment into a number of moving fundamental solitons which fly tangentially off the ring, as expected. For both vortices and soliton rings, we established the existence of propagation distance minimum and of beam power threshold.

Acknowledgement

Work at the Institute of Physics is supported by the Ministry of Science, under the Project OI 141031.

References

[1] Y.S. Kivshar, G.P. Agrawal, Optical Solitons, Academic Press, San Diego, 2003.
[2] B.A. Malomed, D. Mihalache, F. Wise, L. Torner, J. Opt. B 7 (2005) R53.
[3] M. Soljačić, S. Sears, M. Segev, Phys. Rev. Lett. 81 (1998) 4851.
[4] M. Soljačić, M. Segev, Phys. Rev. E 62 (2000) 2810.
[5] A.S. Desyatnikov, Y.S. Kivshar, Phys. Rev. Lett. 87 (2001) 033901.
[6] A. Desyatnikov, Y. Kivshar, L. Torner, Optical vortices and vortex solitons, in: E. Wolf (Ed.), Progress in Optics, vol. 47, North-Holland, Amsterdam, 2005, p. 219.
[7] Y.V. Kartashov, L.-C. Crasovan, D. Mihalache, L. Torner, Phys. Rev. Lett. 89 (2002) 273902.
[8] L.-C. Crasovan, Y.V. Kartashov, D. Mihalache, L. Torner, Y.S. Kivshar, V.M. Pérez-García, Phys. Rev. E 67 (2003) 046610.
[9] D. Mihalache, D. Mazilu, L.-C. Crasovan, B.A. Malomed, F. Lederer, L. Torner, J. Opt. B 6 (2004) S333.
[10] A.S. Desyatnikov, Y.S. Kivshar, Phys. Rev. Lett. 88 (2002) 053901.
[11] A.S. Desyatnikov, Y.S. Kivshar, J. Opt. B 4 (2002) S58.
[12] D. Mihalache, D. Mazilu, L.-C. Crasovan, B.A. Malomed, F. Lederer, L. Torner, Phys. Rev. E 68 (2003) 046612.
[13] O. Bang, W. Krolikowski, J. Wyller, J.J. Rasmussen, Phys. Rev. E 66 (2002) 046619.
[14] S. Lopez-Aguayo, A.S. Desyatnikov, Y.S. Kivshar, S. Skupin, W. Krolikowski, O. Bang, Opt. Lett. 31 (2006) 1100.
[15] G.F. Calvo, F. Agulló-López, M. Carrascosa, M.R. Belić, W. Królikowski, Europhys. Lett. 60 (2002) 847.
[16] G.F. Calvo, F. Agulló-López, M. Carrascosa, M.R. Belić, D. Vujić, Opt. Commun. 227 (2003) 193.
[17] W.J. Firth, D.V. Skryabin, Phys. Rev. Lett. 79 (1997) 2450.
[18] D.V. Skryabin, W.J. Firth, Phys. Rev. E 58 (1998) 3916.